Electrochemical impedance spectroscopy using exponentially-rising voltage steps. (I) Analysis of a model electrical circuit

P. Millet

Institut de Chimie Moléculaire et des Matériaux d'Orsay, UMR CNRS n° 8182, Université Paris Sud 11, 15 rue Georges Clémenceau, 91405 Orsay cedex France

Electrochemical impedance spectroscopy (EIS) is commonly used by electrochemists to analyze multi-step reaction paths occurring at electrode/electrolyte interfaces. Since the kinetics of individual reaction steps is usually a function of electrode potential, the impedance of the interface is measured for different but constant potential values. In most cases, impedance diagrams are obtained from harmonic analysis: a surimposed low amplitude (typically 5-10 mV) ac potential modulations or alternatively, a low amplitude (typically a few mA) ac galvanostatic modulation, is used as perturbation. However, according to the theory of linear and time invariant systems, harmonic analysis should be restricted to the analysis of linear and reversible processes. To a certain extend, the problem of linearity can be circumvented by reducing the amplitude of the modulation. But that does not help to solve the problem of irreversibility. For example, a significantly large hysteresis is observed during the electro-insertion of hydrogen into palladium or palladium alloy electrodes. This is a clear indication that non-linear phenomena are taking place and therefore, the use of harmonic analysis should be prohibited because the system does not fulfill the requirements of linearity and time invariance imposed by the theory of systems. There is therefore a need to use non-alternating perturbations. The purpose of this paper is to report on the measurement of impedance spectra from exponentially-rising voltage-step excitations. This is a methodology-oriented communication. In the first part of the paper, an electrical circuit containing only electrical resistances and capacitances is used as a model system to explain how impedance diagrams can be obtained from such non-harmonic perturbations. In the second part of the paper, the methodology is extended to the electro-insertion of hydrogen in palladium foils.

Key words: Impedance spectroscopy, Voltage excitation, Electrical circuit

INTRODUCTION

In chemical science, the term "kinetics" is usually making reference to the rate (expressed in $mol.s^{-1}$ or in $mol.s^{-1}.cm^{-2}$ when the active surface is known) at which a given process is occurring. But raw kinetic data, when properly analyzed, carry detailed information on chemical or electrochemical multistep reaction mechanisms. From a practical viewpoint time domain analysis and modeling of raw data is not always trivial because kinetic features of individual steps are usually convoluted. Alternatively, frequency-domain (Fourier) analysis offers the possibility of measuring transfer functions which unambiguously characterize reaction mechanisms and gives access to the rate parameter associated with each reaction step. Electrochemical transfer functions measured at electrode/electrolyte interfaces relate potential perturbations to associated current responses. Such (complex) transfer functions are thus electrical impedances (or conversely, admittances). Harmonic analysis (using sine-wave perturbations) is certainly the most popular way of measuring electrochemical impedances [1] but miscellaneous signals (such as white noise [2], square-waves [3] or multiple sine waves [4]) have also been used as input potential or current perturbations. Other techniques such as current interrupt [5] and alternating current (ac) voltammetry, which was invented in the 1950s [6-9], can also be used for quantitative evaluation of the mechanisms of electrode processes. Conventionally, with the ac technique, a small amplitude sinusoidal potential with a frequency of 10 Hz-100 kHz is superimposed onto the triangular waveform used in dc cyclic voltammetry, and either the total ac response or the dc, fundamental, and higher harmonic are then measured as a function of dc potential and frequency. Garland *et al.* used the technique to study the UPD adsorption of Bi^{3+} at gold electrodes [10]. The technique has also been extended to the combination of cyclic voltametry and surimposed square waves, triangles, sawtooth waveforms or non-harmonically related sine components [11]. However, according to the theory of linear and time invariant systems, the use of wave (alternating) perturbations is restricted to the

---

* To whom all correspondence should be sent:
E-mail: pierre.millet@u-psud.fr

characterization of linear systems and reversible transformations. To a certain extend, the problem of linearity can be circumvented by reducing the amplitude of the surimposed modulation. But that does not help to solve the problem of irreversibility. For example, a significantly large hysteresis is observed during the electro-insertion of hydrogen in palladium or palladium alloys. This is a clear indication that non-linear phenomena are taking place and therefore, the use of harmonic analysis should be prohibited because the system does not fulfill the requirements of linearity and time invariance imposed by the theory of systems. To investigate the dynamic features of such systems, there is therefore a need to use non-alternating perturbations. Potential steps are appropriate signals for the measurement of impedances at electrode/electrolyte interfaces where irreversible processes are taking place because their first time-derivative is strictly positive (rising up step) or negative (rising down step). Application of potential steps to such systems offers the possibility to study separately back and forth transformations. The concept has already been proposed to analyze the electrochemical hydriding reactions of palladium in two-phase domains [12] but few details were given concerning the methodology used for the measurements. A similar concept based on the application of "pressure steps" has also been used to analyze gas-phase reactions [13]. The purpose of this paper is to describe the measurement of impedance diagrams from potential steps. This is a methodology-oriented communication and we focus primarily on the constraints and criteria of measurements in the context of new data acquisition electronics that became available during the last few years. In the first part of the paper, an electrical circuit containing only electrical resistances and capacitances is used as a model system. This is a simple case because experiments are very brief (a few milliseconds long). As a result, sampling conditions and data treatment procedures are easy to manage and impedance diagrams easy to obtain. In the second part of the paper, the methodology is extended to the study of a more complicated case, the electro-insertion of hydrogen in palladium foils.

EXPERIMENTAL

Experimental setup

A computer-controlled Radiometer Analytical PGZ 402 potentiostat-galvanostat has been used to apply voltage excitations. In addition, an Agilent DSO 6032 A (2 channels, 300 MHz) oscilloscope

has been used to sample the potential and current transients. Short (10 cm long) electric cables were used to minimize parasite impedance losses.

Electrical circuit

The model electrical circuit used for the experiments is pictured in Fig 1. Two parallel RC circuits (R_1, C_1 and R_2, C_2) are connected in series. The time constants of each sub-circuit ($\tau_1 = R_1.C_1 = 2.35 \times 10^{-5}$ s and $\tau_2 = R_2.C_2 = 10^{-2}$ s) differ by a factor of $\tau_2/(\tau_1 = 425$, and each sub-circuit has quite different dynamic features. A third resistance R_0 is connected in series.
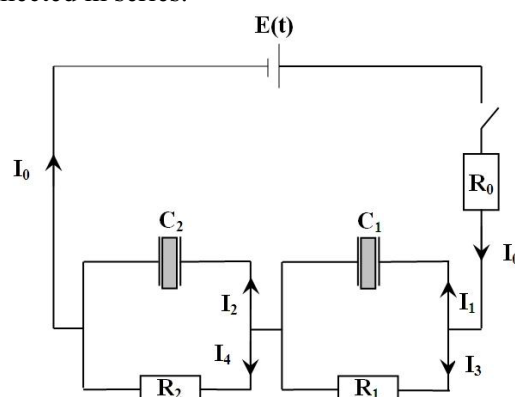

Fig. 1. Model electrical circuit. $R_0 = 12100$ Ω; $R_1 = 4990$ Ω; $C_1 = 4.7 \times 10^{-9}$ F; $R_2 = 10000$ Ω; $C_2 = 1 \times 10^{-6}$ F. E(t) = voltage excitation. I_0, I_1, I_2, I_3 and I: current responses.
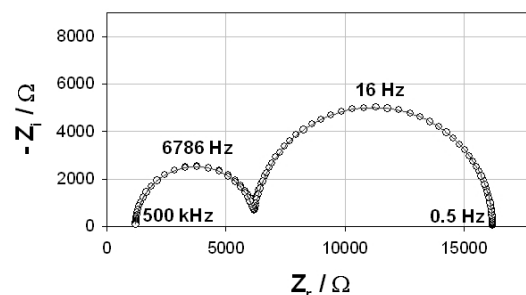

Fig. 2. Impedance diagram of the electrical circuit of Fig 1.(o) experimental (sine wave perturbation); (—) calculated from Eq. (1).

The analytical impedance of the electrical circuit of Fig. 1 is given by equation (1) where $\omega = 2\pi f$ is the pulsation in rad.s^{-1} and f is the frequency in Hz:

$$Z(\omega) = R_0 + \cfrac{1}{j\omega C_1 + \cfrac{1}{R_1}} + \cfrac{1}{j\omega C_2 + \cfrac{1}{R_2}} \quad (1)$$

The experimental impedance diagram measured with the Radiometer potentiostat using sine wave potential perturbations is plotted in Nyquist coordinates in Fig. 2. The measure was made at a constant voltage of 0 V with a 5 mV sur-imposed ac perturbation. The model impedance diagram

339

obtained from Eq. (1) is also plotted for comparison. There is a good overall agreement over the entire frequency range, indicating that the values of R_0, R_1, R_2, C_1 and C_2 given in the caption of figure 1 are known with a sufficiently good accuracy and that the signal-to-noise ratio is appropriately high. The time constant of the two RC circuits are significantly different and the impedance of each sub-circuit (a semi circle along the real axis) are well separated in frequency. The impedance of the first sub-circuit (R_1, C_1) with the lowest time constant appears in the high frequency range and the impedance of the second sub-circuit (R_2, C_2) appears in the low frequency range. The characteristic pulsations ω_c (in rad.s^{-1}) at the top of each semi-circle is related to each time constant: $\omega_{ci} = 2\pi f_{ci} = 1/\tau_i$. where f_{ci} is the corresponding characteristic frequency (in Hz or s^{-1}). Practical conditions required for obtaining impedance diagrams from potential step excitations are discussed in the following sections.

THEORY

Linear and time invariant systems (LTIS)

In the followings, the implicit variable is time (t) throughout. System theory analyzes the relationships between any given input i(t) and the corresponding output o(t). A system is said to be linear and time invariant when the following conditions are satisfied:

(i) causality:

$$i(t), o(t) = 0 \quad \forall t < 0 \qquad (2)$$

(ii) linearity:

$$\alpha_1 i_1(t) + \alpha_2 i_2(t) \rightarrow \beta_1 o_1(t) + \beta_2 o_2(t) \quad (3)$$

where α_1, α_2, β_1 and β_2 are scalars.

(iii) time invariance:

$$i(t - \tau) \rightarrow o(t - \tau) \qquad (4)$$

where τ is the time shift.

Let *h*(t) be the output obtained when the unit impulse (Dirac) function δ(t) is applied as input. h(t) is called the impulse response :

$$\delta(t) \rightarrow h(t)$$

$$(5)$$

The theory of LTIS demonstrates that for systems satisfying conditions (2), (3) and (4), the output o(t) is related to the convolution product of the input i(t) by h(t) :

$$o(t) = \int_{-\infty}^{+\infty} i(\tau) h(t - \tau) d\tau = i(t) * h(t) \quad (6)$$

Complex exponentials remain frequency unaltered when passing through LTIS. Only amplitude modulations and phase shifts occur. i(t) and o(t) can thus be adequately expressed on the

basis of complex exponentials. This operation is called Fourier transformation:

$$G(f) = FT[g(t)] = \int_{-\infty}^{+\infty} g(t) e^{-j\omega t} dt \quad (7)$$

where f is the frequency in Hz, $\omega = 2\pi f$ is the pulsation in rad.s^{-1}, and FT[g(t)] is the Fourier transform of g(t).

An interesting property of the Fourier transformation is that the convolution product (6) in the time (direct) domain is simply an algebraic product in the Fourier (frequency) domain:

$$FT[i(t) * h(t)] = FT[i(t)] \bullet FT[h(t)] = FT[o(t)] \quad (8)$$

The FT of the impulse response h(t) is called the transfer function of the system:

$$FT[h(t)] = H(f) = \int_{-\infty}^{+\infty} h(t) e^{-j\omega t} dt \quad (9)$$

Thus, for a LTIS, the general relationship between input i(t) and output o(t) is a convolution product in the time-domain and an algebraic product in the Fourier domain. According to Eq. (8), the transfer function H(f) can be obtained in principle by taking the ratio of the FTs of any pair {i(t); o(t)}, ie : H(f) = FT{o(t)}/FT{i(t)}. This is possible as long as the denominator is non-zero at the frequencies of interest. It turns out that this is the case for electrical and electrochemical systems for which the input i(t) is the electric potential E(t) and the response o(t) is the current I(t). The associated transfer function is a complex impedance Z(ω):

$$Z(\omega) = \frac{E(\omega)}{I(\omega)} \qquad (10)$$

E(ω) is the Fourier Transform (FT) of the voltage excitation E(t) in Volt and I($\square$) is the FT of the current response in Amp.

Voltage excitations

Electrical potential steps E(t) generated by commercial potentiostats are not true Heaviside steps. In order to avoid dumping effects, E(t) has usually a finite rising-time and is, instead of a true step, an exponential function rising to a maximum value (Fig. 3), the analytical expression of which is:

$$E(t) = a. [1 - exp(-b.t)] \qquad (11)$$

where a is the amplitude in V and b = $1/\tau$ in s^{-1} (τ is a time constant in s). This is why in this paper, such signals are called "exponentially-rising voltage-step excitations". Results were obtained using a PGZ402 potentiostat from Radiometer, with a mean time constant τ = 1/b = 6.424x10^{-5} s (when no filter is used). Experimental voltage excitations generated by the potentiostat were found to be reproducible

within ± 0.05 % from one experiment to the other. The frequency content of such voltage excitations can be determined by taking the Fourier transform (FT) of Eq. (11). A convenient way to do that is to calculate the Laplace transform (LT) and then explicit the transformation variable $s = j\omega$:

$$LT\{E(t)\} = a\int_0^{+\infty} \left(1 - e^{-bt}\right)e^{-pt}\, dt = a\left[\frac{1}{p} - \frac{1}{p+b}\right] = \frac{ab}{p^2 + bp}$$

$$(12)$$

$$FT\{E(t)\} = LT\{E(t), p = j\omega\} = \frac{ab + j0}{-\omega^2 + j\omega b} \quad (13)$$

Eq. (13) is the general solution except for $\omega = 0$ for which ($\delta (t)$ is the Dirac function):

$$FT\{E(t), \omega = 0\} = \delta(t)\frac{a}{2} \quad (14)$$

In conventional harmonic analysis, sine wave functions of similar amplitudes are used to measure the impedance of the system over the entire frequency range of interest on a frequency-to-frequency basis. As can be seen from Eqs. (13) and (14), the energy content of an exponentially-rising voltage-step excitations is inversely proportional to the frequency. This is a limitation of the technique because the energy of the signal decreases as the frequency increases. Therefore, the amplitude of the excitation must be sufficiently large and the apparatus used to measure the current response must be sufficiently sensitive to accurately sample the signals.

RESULTS AND DISCUSSION

Experimentally, the problem to solve consists in the measurement of the impedance of a given system of interest by using such smooth voltage excitations as perturbation. In the first part of this paper, the system under consideration is the electrical circuit of Figure 1. This is a low noise system and equilibrium is reached within a few tens of milliseconds. In the second part of the paper, the system will be a noisier electrode/electrolyte interface for which equilibrium is reached within only a few seconds. The same methodology is used to characterize both systems. In a typical experiment, two transient signals are sampled : the rising voltage excitation E(t) and the associated current response I(t). To determine the unknown impedance of the electrical circuit there are two options: (i) frequency-domain analysis : the Fourier transform of both E(t) and I(t) are calculated and the ratio of the two FTs is taken as shown in Eq. (10), yielding the impedance Z(ω) of the circuit; this is the most straightforward method; (ii) time-

domain analysis: a model circuit impedance Z(ω) is postulated; then, I(ω), the FT of the current response to the voltage excitation is calculated from Eq. (10): I(ω) = E(ω) / Z(ω); then, model I(t) is calculated from I(ω) by inverse Fourier transformation and used to fit transient experimental current I(t); parameters of the model impedance Z(ω) are iteratively adjusted to minimize the difference between model and experimental I(t) in order to determine the exact characteristic of circuit components. This second approach is more difficult to implement than the first one but can sometimes be more efficient and even more accurate. It can also be automated. The two approaches are detailed in the followings. The circuit of Fig. 1 of known impedance is used as a model system to describe the methodology and to evaluate the role of data sampling and data filtering on the quality of the resulting impedance.

Frequency-domain analysis

Solution to the convolution equation in the frequency domain. The impedance diagram of the circuit of Fig. 1 can be obtained directly from frequency-domain analysis of experimental data using Eq. (15):

$$Z(\omega) = \frac{E(\omega)}{I_0(\omega)} \quad (15)$$

where E is the voltage excitation in Volt, I_0 is the current response of the cell in A, and ω is the pulsation in rad.s^{-1}. E(ω) denotes the Fourier transform of the voltage excitation E(t), and $I_0(\omega)$ denotes the Fourier transform of the current response I(t).

Sampling conditions and data treatment. In order to calculate the impedance diagram, there is a need to sample both transient signals : voltage excitation and current response. The Fourier transform of the discrete transients can then be calculated and the ratio yields the desired impedance diagram. The sampling rate must respect the Nyquist criterion which states that the signal must be sampled more than twice as fast as the highest waveform frequency (f_c). If not, it turns out that all of the power spectral density (PSD) which lies outside of the frequency range $-f_c < f < f_c$ is spuriously moved into that range and the spectrum is corrupted. This phenomenon is called aliasing [14]. According to Fig. 2, the impedance of the circuit reaches the real axis at a frequency value of ≈ 500,000 Hz. Therefore, a sampling rate of one sample every 1 μs (or less) is required. The sampling rate must be maintained until the end of the experiment (20 millisec in the present case). As
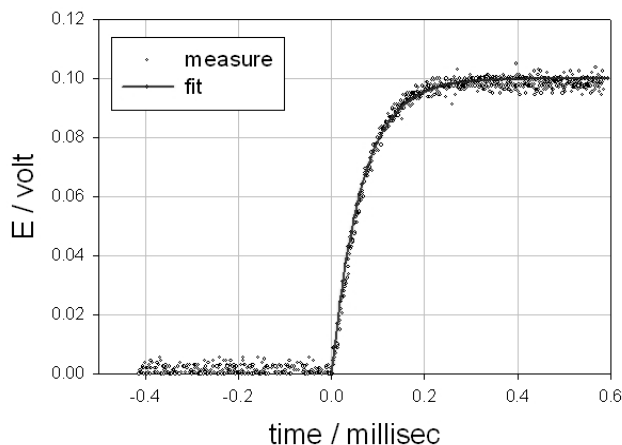
Fig. 3. (o) experimental voltage excitation and (+) best fit using Eq. (11).
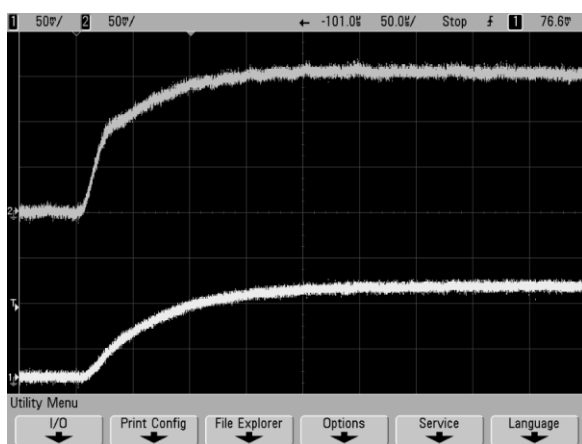

Fig. 4. Experimental voltage excitation (bottom) and current response (top) of the electrical circuit of Fig. 1.

a result, 20,000 datapoints will be collected for each signal, corresponding to a file of only *ca.* 4 Mbytes of floats. The signals displayed on the screen of the oscilloscope at the onset of the step during a typical experiment are shown in Fig. 4 (time scale 0-500 μsec).

Raw data cannot always be used directly. Electronic or numerical filtering using low-pass filters is required prior to Fourier transformation in order to get rid of the polluted high frequency content of raw data [14]. Different filters (available on most potentiostats) can be used for that purpose although they also change the time constant of the step functions. In order to improve the signal-to-noise ratio, a first approach is to use the analytical expression of E(ω) (taken from Eq. (13)) in Eq. (15) instead of sampling the true experimental voltage step. This is justified by the fact that exponentially-rising voltage steps delivered by potentiostat are highly reproducible. Thus, the sampled current response is the only source of noise for the impedance diagram. It should also be noted that, according to Eq. (13), the PSD =
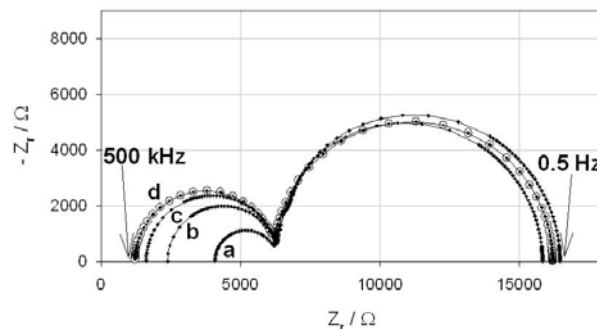

Fig. 5. Impedance diagrams of the circuit of Fig. 1; (o) calculated from Eq. (1); (+) experimental from exponentially-rising voltage-step excitations: (a) $\Delta t = 50$ μs; (b) $\Delta t = 20$ μs; (c) $\Delta t = 10$ μs; (d) $\Delta t = 5$ μs.

$\sqrt{\mathrm{Re}^2\{E(\omega)\} + \mathrm{Im}^2\{E(\omega)\}}$ of the exponentially-rising voltage steps decreases exponentially with frequency. Therefore, a highly sensitive amperemeter and low-pass filtering should be used to obtain well-defined impedance diagrams in the potentially noisiest high-frequency region where widely scattered data-points are obtained otherwise [5].

Comparison of model and experimental impedance values. Impedance diagrams obtained from exponentially-rising voltage-step excitations are plotted in Fig. 5. The theoretical impedance diagram obtained from Eq. (1) is also plotted for comparison. There is a good agreement between both techniques, both in terms of impedance values and frequency content. However, the sampling rate of current responses plays a critical role. A sampling rate of at least one data-point every 5 μs is required to obtain a satisfactory fit (curve d). At 5 μs, a data file of 400 kbytes is obtained and the impedance is calculated within only a few seconds. Therefore, this is achievable using conventional personal computers. If lower sampling rates are used (curves a, b, c), then significant distortions appear in the high frequency range.

Time-domain analysis

Solution to the convolution equation in the time domain. Circuit impedance parameters can also be determined from a time-domain analysis of experimental data. In a typical experiment, the electrical circuit of Fig. 1 is excited by a voltage transient E(t) of any shape. $E_{R0}(t)$ (the voltage of the resistance R_0), $E_{R1}(t)$ (the voltage of the resistance R_1), $E_{C1}(t)$ (the voltage of the capacitance C_1), $E_{R2}(t)$ (the voltage of the resistance R_2), and $E_{C2}(t)$ (the voltage of the capacitance C_2) are the five unknown transient voltages. $I_0(t)$ (the main transient current across the circuit), $I_1(t)$ (the current across capacitance C_1), $I_3(t)$ (the current across

342

resistance R_1), $I_2(t)$ (the current across capacitance C_2) and $I_4(t)$ (the current across resistance R_2) are the five unknown transient currents. By applying Kirchhoff's laws (conservation of charge and) to the circuit of Fig. 1, the following set of five equations is obtained:

$$\frac{1}{C_1} \int_0^t I_1(t)\, dt = R_1 \left[I_0(t) - I_1(t) \right] \quad (16)$$

$$\frac{1}{C_2} \int_0^t I_2(t)\, dt = R_2 \left[I_0(t) - I_1(t) \right] \quad (17)$$

$$E(t) = R_0\, I_0(t) + \frac{1}{C_1} \int_0^t I_1(t)\, dt + \frac{1}{C_2} \int_0^t I_2(t)\, dt \quad (18)$$

$$I_0(t) = I_1(t) + I_3(t) \quad (19)$$

$$I_0(t) = I_2(t) + I_4(t) \quad (20)$$

The system can be solved by use of Laplace transformation. Solutions for the five voltage transients are:

$$E_{R0}(s) = R_0\, I_0(s) \quad (21)$$

$$E_{R1}(s) = R_1 \left[I_0(s) - I_1(s) \right] \quad (22)$$

$$E_{C1}(s) = \frac{I_1(s)}{s\, C_1} \quad (23)$$

$$E_{R2}(s) = R_2 \left[I_0(s) - I_2(s) \right] \quad (24)$$

$$E_{C2}(s) = \frac{I_2(s)}{s\, C_2} \quad (25)$$

Solutions for the five current transients are:

$$I_0(s) = E(s) \left[R_0 + \frac{1}{s\,C_1} \left[\frac{R_1}{R_1 + \frac{1}{s\,C_1}} \right] + \frac{1}{s\,C_2} \left[\frac{R_2}{R_2 + \frac{1}{s\,C_2}} \right] \right]^{-1} \quad (26)$$

$$I_1(s) = I_0(s) \left[\frac{R_1}{R_1 + \frac{1}{s\,C_1}} \right] \quad (27)$$

$$I_2(s) = I_0(s) \left[\frac{R_2}{R_2 + \frac{1}{s\,C_2}} \right] \quad (28)$$

$$I_3(s) = I_0(s) - I_1(s) \quad (29)$$

$$I_4(s) = I_0(s) - I_2(s) \quad (30)$$

Time domain solutions to Eqs. (20-29) can be obtained analytically (this is not always possible, especially as the complexity of the circuit increases) by choosing the shape of the perturbation E(t). Alternatively, solutions can also be conveniently obtained numerically by computing the inverse discrete Fourier transform (IDFT) of Eq. (20-29) for $s = j\omega$. The IDFT h(t) of a signal with a frequency content H(f) is given by:

$$h(t) = \int_{-\infty}^{+\infty} H(f)\, e^{2\pi j f t}\, df \quad (31)$$

The discrete expression of Eq. (31) is :

$$h(t) = \sum_{-\infty}^{+\infty} H(f) \left[\cos(2\pi f t) - j \sin(2\pi f t) \right] \Delta f \quad (32)$$

Transient voltage values. Numerical voltage responses of circuit components (Fig. 1) to E(t) = exponentially-rising voltage-step excitation are plotted in Fig. 6. Data have been obtained numerically by solving Eqs. (21-25) using the circuit impedance of Eq. (1).

The time axis is in logarithmic scale to facilitate the differentiation of the different voltages. The rising voltage excitation E(t) has an amplitude of 0.1 V and reaches its plateau value in less than 0.5 milliseconds. Stationary signals are obtained after *ca.* 2×10^{-2} seconds. At that time, capacitances C_1 and C_2 are charged and their impedance is infinite. A stationary current flows across the series-connected resistances: $\sum_i R_i = R_0 + R_1 + R_2 =$ 16200 Ω. Therefore, the stationary current for t > 10^{-2} s is $I_0 = \dfrac{A}{\sum_i R_i} = 0.1/16200 = 6.17\ \mu A$.

Individual stationary voltages are:

$$E(t) = \lim_{t \to \infty} a \left(1 - e^{-\frac{t}{\tau}} \right) = a = 100\ mV$$

$$E_{R0} = R_0\, I_0 = 7.5\,\text{mV};\ \ E_{R1} = E_{C1} = R_1\, I_0 = 30.8\ \text{mV};$$

$$E_{R2} = E_{C2} = R_2\, I_0 = 61.7\ \text{mV}.$$

According to Kirchhoff's law: E(t) = $E_{R0}(t)$ + $E_{R1}(t)$ + $E_{R2}(t)$.

Therefore, experimental transient voltages of individual circuit components can be fitted with model values. The difference between experimental and model values can be minimized by iteration and the impedance of each circuit component can be adjusted until a complete agreement is obtained between both sets of data.

Transient current values. Numerical current responses of the electrical circuit of Fig. 1 to a exponentially-rising voltage-step excitation E(t) are plotted in Fig. 7. Data have been obtained by solving Eqs. (26-30). Again, the time axis is in logarithmic scale to facilitate the differentiation of the different signals.

For t > 10^{-2} s, the stationary currents are:

$$I_0(t \to \infty) = I_3(t \to \infty) = I_4(t \to \infty) = 6.17\ \mu A$$
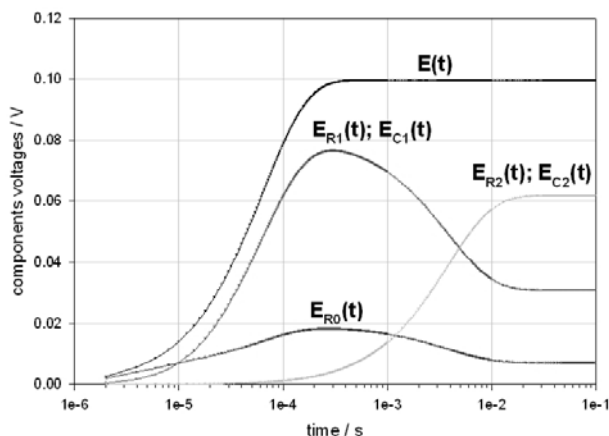
and $I_1(t \to \infty) = I_2(t \to \infty) = 0$.

Fig. 6. Transient voltages responses of the electrical circuit of figure 1 when E(t) = a [1 – exp (-t/τ)]. a= 100 mV. τ = 1/b = 6.424x10⁻⁵ s.
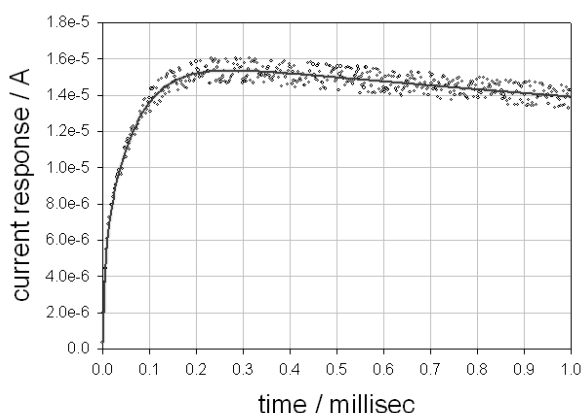

Fig. 7. Transient current responses of the electrical circuit of figure 1 when E(t) = a [1 – exp (-t/τ)]. a= 100 mV. τ = 1/b = 6.424x10⁻⁵ s.

electrical circuits from exponentially-rising voltage-step excitations. When such experiment is carried out, two transient signals are synchronously sampled: the potential excitation E(t) and the current response I(t). To determine the unknown impedance of the electrical circuit there are two options: (i) frequency-domain analysis : the Fourier transform of both E(t) and I(t) are calculated and the ratio of the two FTs is taken using Eq. ω (10), yielding the impedance Z(ω) of the circuit; this is the most straightforward method; (ii) time-domain analysis: a model circuit impedance Z(ω) is postulated; then, the FT I(w) of the current response to a exponentially-rising voltage-step excitation is

Fig. 8. Experimental (o) and model (—) current responses $I_0(t)$ of the circuit of Fig. 1 when a smooth voltage excitation is applied

Model current responses can be used to fit experimental current values, as discussed in the next section.

Comparison of experimental and model values. The experimental current response $I_0(t)$ has been fitted as follows. First, I(ω) has been calculated from Eq. (10): I(ω) = Z(ω) / E(ω). Z(ω) was taken from Eq. (1) and E(ω) was taken from Eq. (13). Second, I(t) was calculated from I(ω) by discrete inverse Fourier transformation. Results obtained for the first millisecond of the experiment are plotted in Fig. 8. There is a good agreement between experimental and calculated transients. Therefore, time-domain analysis of the current response of the interface to a smooth voltage excitation can also be used to determine the impedance of an unknown circuit.

CONCLUSIONS

The work reported here describes a methodology used to determine the impedance of
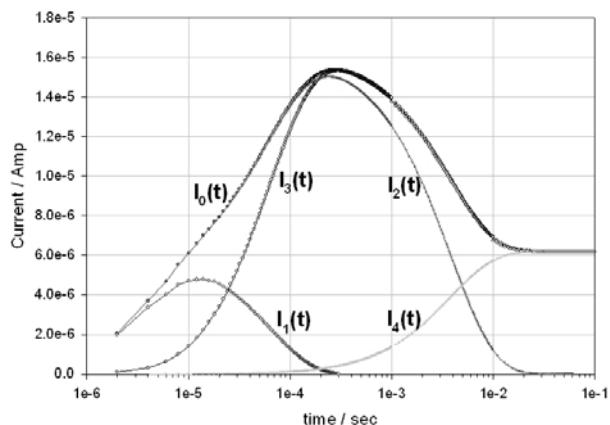
calculated from Eq. (10) : I(ω) = E(ω) / Z(ω); then, model I(t) is calculated from I(ω) by inverse Fourier transformation and used to fit transient experimental current I(t); parameters of the model impedance Z(ω) are iteratively adjusted to minimize the difference between model and experimental I(t) in order to determine the exact characteristic of circuit components. There are two critical problems. First, an appropriate sampling rate must be used. Second, data filtering is required. When these problems are appropriately handled, then correct impedance diagrams are obtained. Therefore, it can be concluded that exponentially-rising voltage-step excitations can be used to measure impedance diagrams of electrical circuits.

REFERENCES

1. L. Schlapbach, A. Züttel, Nature, **414**, 353 (2001).
2. P. Millet, R. Ngameni, Electrochimica Acta 2011, doi: 10.1016/j.electacta.2010.12.106.
3. G. Tsirlina, S. Baronov, F. Spiridonov, M. Rusanova, T. Safonova, O. Petrii, Russ. J. Electrochem., **36**, 1179 (2000).
4. J. Chen, R. Durand, C. Montella, *J. Chem. Phys.,* **91,** 383 (1994).
5. P. Millet, *Electrochem. Commun.,* **7,** 40 (2005).
6. A. Frumkin, in: P. Delahay (Ed.), Advances in Electrochemistry and Electro-chemical Engineering, Vol. 3, Interscience, NewYork, 1963.
7. J. Bockris, J. McBreen, L. Nanis, *J. Electrochem. Soc.,* **112,** 1025 (1965).
8. L. Jacobsen, K. West, *Electrochimica Acta,* **40,** 255 (1995).
9. C. Lim, S. Pyum, *Electrochimica Acta,* **38,** 2645 (1993).
10. E. Barsoukov, J. R. Mac Donald, Impedance Spectroscopy, Theory, Experiment, and Applications, Wiley, 2005.
11. R. Bucur, E. Indren, *Acta Met.*, **35,** 1325, (1987).
12. W. Press, in *Numerical Recipes, the Art of Scientific Computing*, Cambridge University Press: Cambridge, 1986.
13. H. Wiese, K. Weil, IEEE Transactions on Acoustics, Speech, and Signal Processing, **36**(7) July 1988.
14. E. Barsoukov, S. Ryu, H. Lee, *J. Electroanal. Chem.*, **536,** 109 (2002).

ЕЛЕКТРОХИМИЧНА ИМПЕДАНСНА СПЕКТРОСКОПИЯ С ЕКСПОНЕНЦИАЛНО НАРАСТВАЩИ СТЪПКИ НА НАПРЕЖЕНИЕТО
(I) АНАЛИЗ НА МОДЕЛНА ЕЛЕКТРИЧЕСКА СХЕМА

П. Мийе

Институт по молекулярна химия и материали в Орсе, UMR CNRS n° 8182, Университет Париж Юг, ул. Жорж Клемансо 11, 15, 91405 Орсе седекс, Франция

(Резюме)

Електрохимичната импедансна спектроскопия (IES) обикновено се използва от електрохимиците за анализиране на многостепенни реакции, протичащи на фазовата граница електрод/електролит. Понеже кинетиката на отделните стъпки на реакцията обикновено е функция на електродния потенциал, импедансът на фазовата граница се измерва при различни, но постоянни стойности на потенциала. В повечето случаи импедансните диаграми се получават чрез хармоничен анализ: за възбуждане се използва наложена променливотокова модулация на потенциала с ниска амплитуда (типично 5-10 мВ) или галваностатична променливотокова модулация с ниска амплитуда (типично няколко мА). Според теорията на линейните и непроменливи във времето системи обаче, хармоничният анализ следва да бъде ограничен до анализа на линейни и обратими процеси. Проблемът с линейността може да бъде преодолян до известна степен чрез намаляване амплитудата на модулацията. Но това не помага да се разреши проблема с необратимостта. Например, при електро-интеркалацията на водород в електроди от паладий или паладиеви сплави, се наблюдава значителен хистерезис. Това е ясно указание, че протичат нелинейни процеси и следователно хармоничният анализ не може да се използва, защото системата не изпълнява изискванията за линейност и неизменност във времето, наложени от системната теория. Значи трябва да се използва непроменливо възбуждане. Целта на настоящата работа е да се докладва за измерването на импедансни спектри при възбуждане с експоненциално нарастващи стъпки по напрежение. Това съобщение е ориентирано към методологията. В първата част на работата, електрическа схема съдържаща само електрическо съпротивление и капацитет се използва като моделна система, за да се обясни как от такова нехармонично възбуждане може да се получи импедансна диаграма. Във втората част на работата, методологията се разширява до електро-интеркалацията на водород в паладиево фолио.